

The S Segment of Punta Toro Virus (*Bunyaviridae*, *Phlebovirus*) Is a Major Determinant of Lethality in the Syrian Hamster and Codes for a Type I Interferon Antagonist[∇]

Lucy A. Perrone,^{1†} Krishna Narayanan,² Melissa Worthy,^{2‡} and C. J. Peters^{1,2*}

Departments of Pathology¹ and Microbiology and Immunology,² Centers for Biodefense and Emerging Infectious Diseases, University of Texas Medical Branch, Galveston, Texas 77550-0609

Received 24 May 2006/Accepted 5 October 2006

Two strains of Punta Toro virus (PTV), isolated from febrile humans in Panama, cause a differential pathogenesis in Syrian hamsters, which could be a useful model for understanding the virulence characteristics and differential outcomes in other phleboviral infections such as Rift Valley fever virus. Genetic reassortants produced between the lethal Adames (A/A/A) and nonlethal Balliet (B/B/B) strains were used in this study to investigate viral genetic determinants for pathogenesis and lethality in the hamster model. The S segment was revealed to be a critical genome segment, determining lethality with log₁₀ 50% lethal doses for each PTV genotype as follows (L/M/S convention): A/A/A, <0.7; B/A/A, <0.7; A/B/A, 1.5; B/B/A, 2.2; B/A/B, 4.7; A/B/B, >4.7; A/A/B, >4.7; B/B/B, >4.7. In addition, the Adames strain inhibits the induction of alpha/beta interferon (IFN- α/β) in vivo and in vitro and inhibits the activation of the IFN- β promoter. Expression of the PTV Adames NSs protein, encoded by the S RNA segment, inhibited the virus-mediated induction of an IFN- β promoter-driven reporter gene, suggesting that PTV NSs functions as a type I IFN antagonist. Taken together, these data indicate a mechanism of pathogenesis in which the suppression of the type I IFN response early during PTV infection leads to early and uncontrolled viral replication and, ultimately, hamster death. This study contributes to our understanding of *Phlebovirus* pathogenesis and identifies potential targets for immune modulation to increase host survival.

The genus *Phlebovirus* (family *Bunyaviridae*) currently consists of 68 antigenically distinct virus serotypes transmitted by arthropods which are distributed into two groups: the Phlebotomus fever and Uukuniemi groups. Of the known human pathogens in the Phlebotomus fever group, Toscana virus, sandfly fever Naples virus, sandfly fever Sicilian virus, Rift Valley fever virus (RVFV), and Punta Toro virus (PTV) are of greatest public health importance. Sicilian and Naples viruses are responsible for most clinically described “sandfly fever” cases on the European continent, and their distribution extends into northern Africa and as far east as China (30, 36, 38). Toscana virus is an important emerging pathogen in Italy and causes a meningoencephalitic disease in European countries bordering the Mediterranean (10). RVFV causes recurrent epidemics in sub-Saharan Africa and was recently implicated in an outbreak of hemorrhagic fever in the Arabian peninsula (1). RVFV is a major veterinary and human pathogen (26, 27). The most medically important *Phlebovirus* in the Americas is PTV, which has been isolated repeatedly in Panama and Columbia.

Punta Toro virus is transmitted by sand flies and causes an

acute febrile illness lasting 2 to 5 days (5, 30, 31, 37). While up to a 35% seroprevalence has been reported in Panama, little is understood about the clinical spectrum of illness (36). Two strains of PTV isolated from febrile patients in Panama were found to produce a differential pathogenesis in the Syrian hamster, with the PTV-Adames (PTV-A) strain infection causing a RVFV-like illness and death, while animals infected with the PTV-Balliet (PTV-B) strain survived infection (3). As reported in a study by Anderson et al. (3), the PTV-A strain was demonstrated to have a hamster 50% lethal dose (LD₅₀) >1 million-fold lower than that of the PTV-B strain. The finding that PTV-A titers were consistently higher than those of the PTV-B strain at early time points during infection indicates that the PTV-A strain may have a growth advantage by efficiently suppressing the early innate immune response.

The viral family *Bunyaviridae* is composed of 5 genera: *Orthobunyavirus*, *Phlebovirus*, *Nairovirus*, *Hantavirus*, and *Tospovirus*. Virions are enveloped and contain three genomic RNA segments in the negative-sense coding orientation. In phleboviruses, the large (L) segment encodes the RNA-dependent RNA polymerase, the medium (M) segment encodes two surface glycoproteins, G_N and G_C, and a nonstructural protein, NSm. The third small (S) segment of the phleboviruses encodes the nucleoprotein (N) and another nonstructural protein, NSs. The use of genetic reassortants has been critical in determining viral genes involved in host pathogenesis in the *Bunyaviridae* family (14, 18). While the M and L segments of the California serogroup bunyaviruses have been linked to encephalitis in mice, the inhibition of the early innate immune response has been implicated in the pathogenesis of RVFV infection in mice and is mediated through the NSs gene on the

* Corresponding author. Mailing address: 301 University Blvd., Galveston, TX 77550-0609. Phone: (409) 772-0090. Fax: (409) 747-0602. E-mail: cjpeters@utmb.edu.

† Present address: Influenza Division, Immunology and Pathogenesis Branch, MS G-16, CCID, NCIRD, Centers for Disease Control and Prevention, 1600 Clifton Road, N.E., Atlanta, GA 30033.

‡ Present address: Texas A&M University, College of Veterinary Medicine, Department of Veterinary Pathobiology; MS 4467, College Station, TX 77843.

[∇] Published ahead of print on 18 October 2006.

TABLE 1. PTV reassortant genotyping primers

Virus genome segment	Vc primer sequence	Vs primer sequence (product size [bp]) for virus:	
		Adames	Balliet
L	CTTCTCTTTGGCATATAGCAT	TCACTTGCAGATCTTACTTTCTTC ATGA (250)	GGATGTTTGTAGTCTTGACCT CAGT (350)
M	ACACAAAGACCGGCACATC TCAC	ACCTTTATAAAGCACAGAGTAAC TGCC (150)	GTGCATATGAAGACCATCC AATCC (255)
S	AGCCAGCAGATGTGTTCTC TGAG	AAATTCAAAAACACACTAACACTG AAACC (510)	TTTTTTTTATTTTTTGTGTG TTTATTTTATA (480)

S segment (9, 25, 34, 39). To expand our understanding of *Phlebovirus* pathogenesis, we utilized genetic reassortants produced between the PTV-A and PTV-B strains to determine segment-associated virulence factors in the hamster model (3, 13). This study reports the finding that the S RNA segment of the PTV genome is a critical factor determining virulence in hamsters and that an inhibition of an early induction of alpha/beta interferon (IFN- α/β) by the PTV-A strain contributes to the lethality in hamsters.

MATERIALS AND METHODS

Viruses and cells. Manipulations of all viruses and their RNA were performed in approved BSL-2 and ABSL-2 facilities. PTV strains (PTV-Adames_[VeroE6 (9)] and PTV-Balliet_[SM(12), VeroE6(3)]) were obtained from the World Arbovirus Reference Collection at UTMB (courtesy R. B. Tesh). Virus stocks and reassortant virus progeny (described below) were generated and propagated in Vero E6 cells. Newcastle disease virus and vesicular stomatitis virus (VSV) were kindly provided by S. Baron (UTMB), and Sendai virus (SEN; Cantell strain) was obtained from Charles River Laboratory (Wilmington, MA). Vero E6 cells were maintained in Earle's minimal essential medium (EMEM) supplemented with antibiotics and 10% fetal calf serum (FCS). 293 cells were grown in Dulbecco's minimal essential medium supplemented with antibiotics and 10% FCS. Chinese hamster (*Cricetulus griseus*) ovary (CHO) cells (CHO-K1; ATCC, Manassas, VA) were maintained in Ham's F-12 media supplemented with antibiotics and 10% FCS.

Generation of PTV reassortants. Confluent monolayers of Vero E6 cells were coinoculated with both PTV-Adames (A/A/A [L/M/S convention] genotype) and Balliet (B/B/B) strains at a multiplicity of infection (MOI) of 3 for each strain, and cells were observed for cytopathic effect (CPE). Cultures were harvested for virus isolation 72 h postinfection (p.i.) or when CPE reached 75%. Plaque assays were performed, and 309 well-separated polymorphic plaques were selected with a cotton-plugged, glass Pasteur pipette for genotype analysis. Agar plugs containing a single plaque were resuspended in 100 μ l EMEM, supplemented with 5% fetal bovine serum. Half of this suspension was used to infect confluent Vero E6 cells in a 24-well plate, and the remaining portion was frozen at -80°C . RNA was extracted at the time point when CPE was observed, and genotyping reverse transcription (RT)-PCR was utilized to screen for PTV reassortants. Reassortant progeny were identified by multiplex RT-PCR and triple plaque purified from the original F₁ plaque plug. Reassortant genotypes were confirmed by partial genome sequencing.

Genotyping PTV reassortants. Multiplex RT-PCR utilizing 3 primers, 2 primers specific to either the Adames or Balliet strain (Vs) and a primer specific to both strains (Vc), per genomic segment were used to identify reassortant progeny (Table 1). Genotyping primers were designed based on sequences available through GenBank (accession numbers K02736 [16], DQ363406, DQ363407, M11156 [17], DQ363408, and DQ363409). The PTV sequence data generated in these studies were submitted to GenBank (see "Nucleotide sequence accession numbers" below). Each genome segment was screened for in separate reactions containing both the strain-specific Vs primers and the corresponding Vc primer for that segment. Viral RNA was extracted from infected Vero E6 cultures using TRIzol reagent (Invitrogen Corp., Carlsbad, CA) as directed. Reverse transcription was performed using 500 ng RNA with virus-specific primers or random hexamers (Promega Corp., Madison WI) and Superscript II or Superscript III enzymes (Invitrogen) according to the manufacturer's protocol. PCR components consisted of 4 μ l cDNA, 100 ng each primer, 2.5 U *Taq* polymerase (Promega), 10 mM Tris-HCl (pH 9.0), 50 mM KCl, 0.1% Triton X-100, and 1.5

mM MgCl₂ for a total 50- μ l volume per reaction. PCR conditions were 95°C for 5 min, followed by 30 cycles of 95°C for 40 s, 55°C (S segment) or 60°C (M segment) or 62°C (L segment) for 30 s, 72°C for 35 s, and a final 10-min extension at 72°C. PCR fragments were observed on 2% agarose gels containing ethidium bromide (data not shown).

Production of hamster IFN- α/β . Syrian hamster (*Mesocricetus auratus*) (Harlan Labs, Indianapolis, IN) IFN- α/β was produced from primary cells for use as a standard in these assays. Briefly, embryos were obtained 9 days postimpregnation and were trypsinized and cultured in EMEM supplemented with antibiotics and 20% FCS. Hamster embryo fibroblasts (HEF) (passage 2) were infected with an MOI of 0.01 of Newcastle disease virus and observed for CPE. When 50% cell death was observed in HEF cultures, supernatants were harvested and treated by pH reduction (8). Type I hamster IFN was assayed on CHO cells in 96-well plates using the established VSV plaque reduction method for IFN titration (19). The reciprocal dilution of IFN sample which reduces VSV plaque numbers by 50% represents the number of IFN U/ml in that sample.

Phenotypic characterization of PTV reassortants. The growth of PTV parental and reassortant progeny genotypes were assessed in Vero E6 cells (see Fig. 2), HEFs (see Fig. 3), and 293 cells (data not shown). Confluent monolayers of cells, in T-25 flasks, were infected with PTV reassortants (MOI = 0.01), and growth was measured for two independently derived plaque isolates of each PTV genotype. Culture supernatants were harvested daily until cultures reached 95% cell death. Growth of virus in Vero E6 cultures was measured over time via standard plaque assay on Vero E6 cells in six-well plates. Virus growth titers in HEFs were determined by 50% tissue culture infective dose (TCID₅₀) assay on Vero E6 cells in 96-well plates and scored 4 d p.i.

Infection of hamsters. Animal research was conducted in an approved ABSL-2 facility and in compliance with the Institutional Animal Use and Care and Use Committee at UTMB. Adult female Syrian hamsters (approximately 50 g) were infected intraperitoneally with 100 μ l of respective viral doses prepared in EMEM. Three doses were utilized: 0.7, 2.7, and 4.7 log₁₀ PFU/100 μ l (3). Infection experiments were conducted with two independently derived plaque isolates of each genotype to confirm pathogenic profiles (3 independently derived plaque isolates were utilized for the A/B/A genotype). Animals were observed daily for signs of illness marked by ruffled fur, hunching, and inactivity. Animals that were moribund and some animals which survived viral challenge (day 14 p.i.) were euthanatized by inhalational overdose of Halothane (Halocarbon Labs, River Edge, NJ) and opening of the chest. The serum, liver, lungs, adrenal glands, duodenum, and spleen were removed from selected animals of each genotype for virus titration, immunohistochemistry, and histopathological examination. Immunohistochemistry was performed on tissues from some animals which did not succumb to infection to test for the presence of viral antigen. The PTV inoculum genotype was confirmed by strain-specific multiplex RT-PCR from homogenized livers of animals that succumbed to viral infection. Viral RNA could not be recovered from livers of surviving animals. Animals surviving virus infection were euthanatized 28 days p.i., and serum antibody was quantified by immunoglobulin G capture enzyme-linked immunosorbent assay using PTV antigen produced for these studies (22).

Immunohistochemistry. Formalin-fixed organs were paraffin embedded and sectioned by the UTMB Histopathology Core Facility. Punta Toro polyclonal antibody (courtesy of R. B. Tesh, UTMB) and horseradish peroxidase-conjugated secondary antibody were used to localize virus in tissues (InnoGenex, San Ramon, CA).

Reporter gene assays. 293 cells, grown in 24-well plates, were transfected using TransIT-293 reagent (Mirus, Madison, WI) according to the manufacturer's instructions. For whole-virus assays, cells were transfected with two plasmids: an IFN- β promoter-driven luciferase (IFN- β -luc) reporter plasmid (a gift from R. Lin, McGill University) and a cytomegalovirus (CMV) promoter-driven β -galac-

TABLE 2. Infection of Syrian hamsters with PTV reassortants

Genotype ^a	No. infected	No. dead	Mortality (%) ^b	No. dead/no. infected (MTD[days]) at virus dose (log ₁₀ PFU) ^b :			Log LD ₅₀
				4.7	2.7	0.7	
A/A/A	60	58	96.7	20/20 (3.1)	20/20 (3.9)	18/20 (4.3)	<0.7
B/A/A	30	28	93.3	10/10 (3.7)	10/10 (4.0)	8/10 (3.4)	<0.7
A/B/A	54	47	87.0	10/17 (3.8)	17/17 (4.8)	20/20 (5.8)	1.5
B/B/A	30	19	63.3	8/10 (5.0)	8/10 (7.0)	1/10 (7.0)	2.2
B/A/B	30	9	30.0	5/10 (6.0)	3/10 (5.3)	1/10 (6.0)	4.7
A/B/B	30	1	3.3	1/10 (6.0)	0/10	0/10	>4.7
A/A/B	30	0	0.0	0/10	0/10	0/10	>4.7
B/B/B	60	0	0.0	0/15	0/15	0/15	>4.7

^a L/M/S RNA segment convention.

^b Cumulated for all three dose groups.

tosidase (CMV-β-Gal) reporter plasmid as an internal control. After 6 h post-transfection at 37°C, the cells were mock infected or infected with PTV-Adames or PTV-Balliet strains at an MOI of 3. Sendai virus (Cantell strain) was used as a positive control, and assays were performed in triplicate. Eighteen hours postinfection, the cells were harvested and lysed in reporter lysis buffer (Promega, Madison, WI), and assays were performed. For expression studies, the cDNAs encoding the PTV Adames and Balliet NSs open reading frame (ORF) region were cloned into the pcDNA3.1 HisA myc (Invitrogen, San Diego, CA). The Ebola virus VP35 gene (a known IFN antagonist) (6) was also cloned into the pcDNA 3.1 HisA myc and was used as a positive control. Empty vector was used as a negative control. 293 cells were transfected with the indicated expression plasmids along with the IFN-β-luc and CMV-β-Gal reporter plasmids as described above. Twenty-four hours later, the cells were infected with Sendai virus using 100 hemagglutinin U/ml of culture. Eighteen hours postinfection, the cells were lysed with reporter lysis buffer, and assays were performed. The luciferase and β-Gal assays were performed using Promega assay kits according to the manufacturer's recommendations. Firefly luciferase activities were normalized to the corresponding β-galactosidase activities to calculate the relative induction.

Nucleotide sequence accession numbers. The PTV sequence data generated in these studies were submitted to GenBank and assigned accession numbers DQ363406, DQ363407, DQ363408, and DQ363409.

RESULTS

The S segment of Punta Toro virus is a critical determinant of lethality in the Syrian hamster. To reveal the viral genetic factors for PTV virulence in vivo, we utilized genetic reassortants produced between the hamster-lethal Adames (PTV-A) and nonlethal Balliet (PTV-B) strains to determine the respective roles of each viral RNA segment in pathogenesis. PTV reassortants were produced in Vero E6 cells following coinfection with PTV-A and PTV-B strains, and the genotype was confirmed by multiplex RT-PCR screening using specific primers (Table 1) as described in Materials and Methods. Reassortants were partially sequenced to confirm the genotype (data not shown). Adult female Syrian hamsters were infected with PTV reassortants or parental PTV-A (A/A/A) (L/M/S convention) or PTV-B (B/B/B) strains. As expected, animals infected with PTV-A strain (A/A/A) exhibited high mortality (97% cumulated over all three virus doses) and the lowest median time to death (MTD) (3.1 days) at each dose compared to other PTV genotypes. Those animals infected with PTV-B did not succumb to infection (Table 2). All PTV genotypes which contained the PTV-A S RNA segment were found to be highly lethal. The B/A/A genotype was the most lethal reassortant genotype, killing 28 of 30 animals and having an LD₅₀ of 0.7, followed by the lethal genotypes A/B/A and B/B/A which killed

87% and 63% of infected animals and had LD₅₀s of 1.5 and 2.2, respectively. Interestingly, the A/A/B genotype, like the B/B/B genotype, was not lethal at any inoculum dose tested, and the A/B/B and B/A/B genotypes were highly attenuated. As demonstrated by the B/B/A and A/A/B genotypes, these data show that the PTV-A S segment contributes significantly to lethality in hamsters and indicates that the S segment encodes a viral gene product important in hamster pathogenesis.

All animals that succumbed to infection with a lethal PTV genotype exhibited hemorrhagic necrosis and epithelial sloughing of the duodenum (Fig. 1A and B). Gross observation of the gastrointestinal tract of these hamsters reveals a dark red and swollen appearance indicative of severe hemorrhage; however, the duodenum is the only site of viral infection and tissue sloughing along the length of the intestine. Viral antigen is detected in columnar epithelial cells along the villi and detection of viral antigen precedes the onset of necrosis along the duodenum (Fig. 1C). Viral antigen can be detected up to 14 d p.i. in animals infected with nonlethal genotypes and sacrificed for examination; this is associated with some villous tip sloughing (not shown), although it is clear that other animals from the cohort recover from this pathology and survive infection. Intestinal crypts of the small bowel are spared from viral infection and necrosis in all PTV genotype infections (Fig. 1C).

In addition to duodenal histopathology, focal hepatocellular necrosis and associated viral antigen was observed in animals that succumbed to infection regardless of infecting PTV genotype (Fig. 1E). Less-extensive hepatocellular necrosis was observed in PTV-B-infected animals sacrificed early in infection. Splenic hyperplasia with lymphocyte and macrophage activation was also observed in all infected animals; extensive necrosis was not seen except in the B/B/A genotype. Unlike infection with the other lethal PTV genotypes, some animals (9/19) dying after infection with the B/B/A genotype exhibited severe hemorrhagic necrosis of the liver and extensive splenic hyperplasia and red pulp necrosis (Fig. 1G and H). Compared to animals infected with the other three genotypes carrying the S RNA segment from the PTV-A strain, these B/B/A genotype-infected animals exhibited a longer MTD (Table 2). It is possible that the lesions may reflect a longer time in a shock-like state from duodenal hemorrhage because the red pulp splenic lesion and the centrolobular hepatic necrosis resemble those

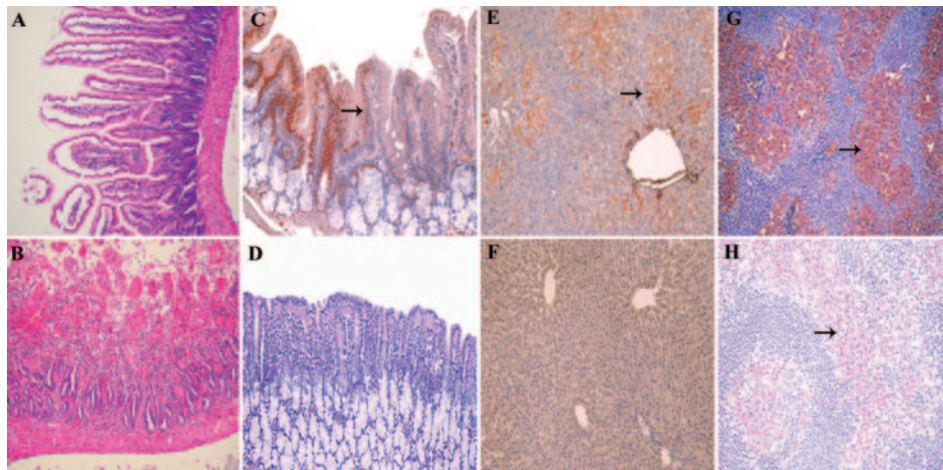


FIG. 1. PTV reassortant histopathology. All animals that succumbed to PTV infection regardless of viral genotype exhibited the same pathology marked by severe duodenal hemorrhagic necrosis. (A) Mock-infected hamster duodenum showing normal histology and villous architecture (hematoxylin and eosin [H&E] stain). (B) Duodenum from an A/A/A genotype infected hamster (died 3 days p.i.). All animals infected with lethal genotypes exhibited severe hemorrhagic necrosis of the epithelium (H&E stain). (C) Animals that did not succumb to infection with nonlethal PTV genotypes exhibited some mild villous tip sloughing and the presence of viral antigen (in red, arrow) in the duodenum, as represented by this section from a hamster infected with the B/B/B genotype (animal was euthanized 14 days p.i.). (D) Mock-infected duodenum (stained for the presence of viral antigen as in panels C, E, and F [H&E counterstain]). (E) PTV antigen (in red, arrow) can be detected in livers of animals infected with lethal genotypes (A/A/A infected hamster, died 4 days p.i.). (F) PTV antigen is not detected in livers from animals infected with nonlethal genotypes (B/B/B infected hamster euthanized 14 days p.i.). (G) Some animals that succumbed from infection with the B/B/A genotype exhibited hepatomegaly due to marked zonal hemorrhagic necrosis (arrow) (H&E stain). (H) Severe red pulp necrosis (arrow) and lymphoid hyperplasia were also observed in some animals infected with the B/B/A genotype (H&E stain).

seen in protracted human shock. All PTV genotypes exhibit the same overall tissue tropism.

PTV reassortant genotypes exhibit different growth properties in IFN- α/β -competent cells. The growth of parental PTV-A and PTV-B and reassortant viruses was assessed in Vero E6 cells (Fig. 2). Although some genotypes displayed slightly different growth patterns, they were not found to be statistically significant in duplicate experiments (data not shown). Each genotypic combination is fully viable and capable of efficient replication in a cell line unable to produce interferon (Fig. 2). We also confirmed the lack of important differ-

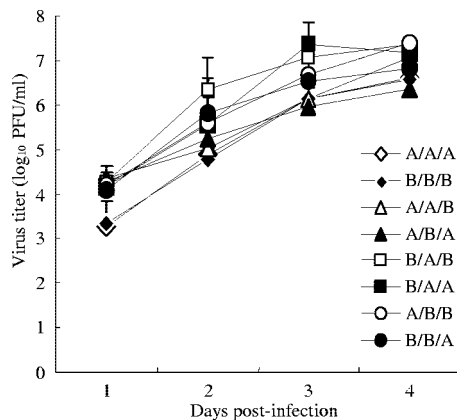


FIG. 2. Characterization of PTV reassortants in IFN- α/β incompetent cells. Confluent monolayers of Vero E6 cells were infected with an MOI of 0.01 of each PTV genotype, and growth of virus was measured over time via standard plaque assay on Vero E6 cells. Growth curves were conducted in duplicate and utilized two independently derived plaque isolates of each PTV genotype.

ences in growth in this study using 293 cells, which are thought to be defective in IFN regulatory factor 7 (32), which would limit the IFN amplification loop in stimulated cells (data not shown). To examine whether the PTV-A S RNA segment confers a growth advantage to PTV reassortant genotypes in IFN- α/β -competent cells, we measured the growth of these viruses in primary HEFs. Cells were infected with each virus genotype at an MOI of 0.01, and titers of virus in the culture supernatant were determined by TCID₅₀ assay on Vero E6 cells. Infections were conducted with two independent plaque isolates of the same PTV genotype and compared to parental genotypes (Fig. 3). Throughout the first 4 days p.i. the PTV-A strain maintains a 100-fold growth advantage over the PTV-B strain. By days 5 and 6, PTV-B titers approach PTV-A levels. The reassortant growth curves are in general bounded by those of the parental strains. If the PTV-B S RNA segment is inserted into the A/A/A genome, the resulting A/A/B genotype replicates much less efficiently and is the only reassortant with even lower titers than the B/B/B parental strain (Fig. 3A). Conversely, the introduction of the PTV-A S RNA segment into the PTV-B genome improved the titers of the B/B/A reassortant in HEFs (Fig. 3A). Similarly, when the PTV-A S RNA segment is expressed in the reassortant A/B/- genotype (Fig. 3B) or the B/A/- genotype (Fig. 3C), the resultant virus grows better than its partner, with the PTV-B segment as the contributor. All of these differences are more prominent early after infection than at later time points. Collectively, these data suggest that PTV-A S segment confers a growth advantage to the virus early during infection in an IFN- α/β -competent system.

The lethal PTV-A strain induces less IFN- α/β in vivo than the nonlethal PTV-B strain. To examine the role of IFN- α/β in

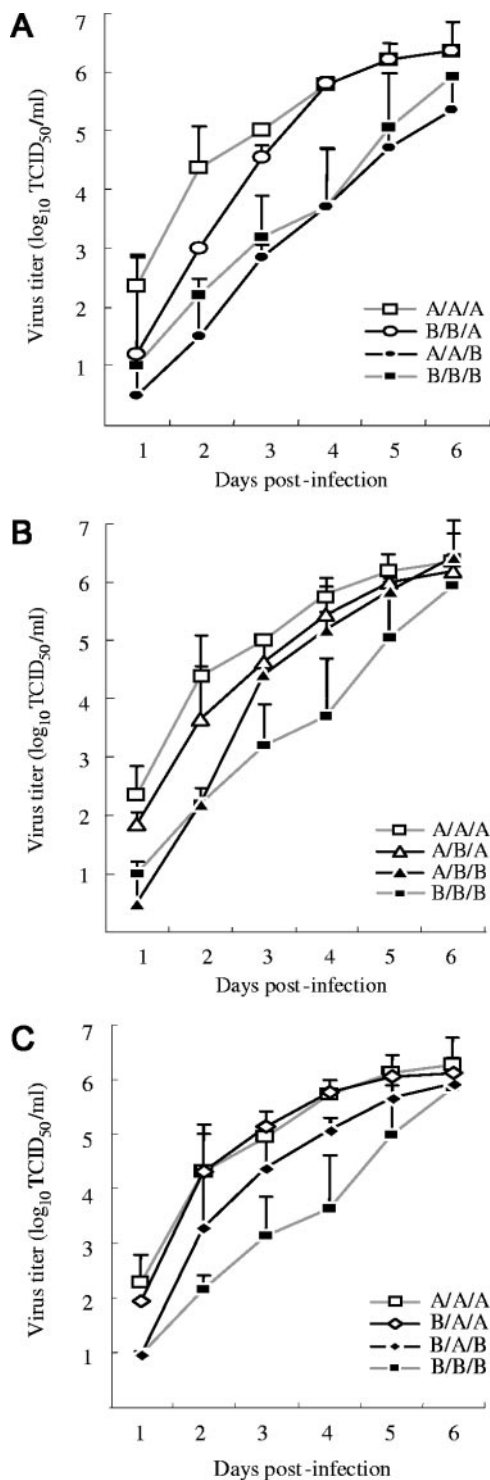


FIG. 3. Characterization of PTV reassortants in IFN- α/β competent cells. Confluent monolayers of primary HEFs in T-25 flasks were infected with an MOI of 0.01 of two independently derived plaque isolates per genotype, and virus growth was measured over time by sampling with medium replacement. Titers were measured by determining the TCID₅₀ on Vero E6 cells. Flasks were sampled with medium replacement until monolayers reached 95% cell death. (A) A/A/A genotype grows to higher titers than B/B/B genotype at all time points, but B/B/B eventually reaches similar titer. Substitution of PTV-B S segment results in a virus (A/A/B) that does not grow as well as B/B/B. The B/B/A genotype exceeds the B/B/B parental genotype, but growth approaches that of the A/A/A ge-

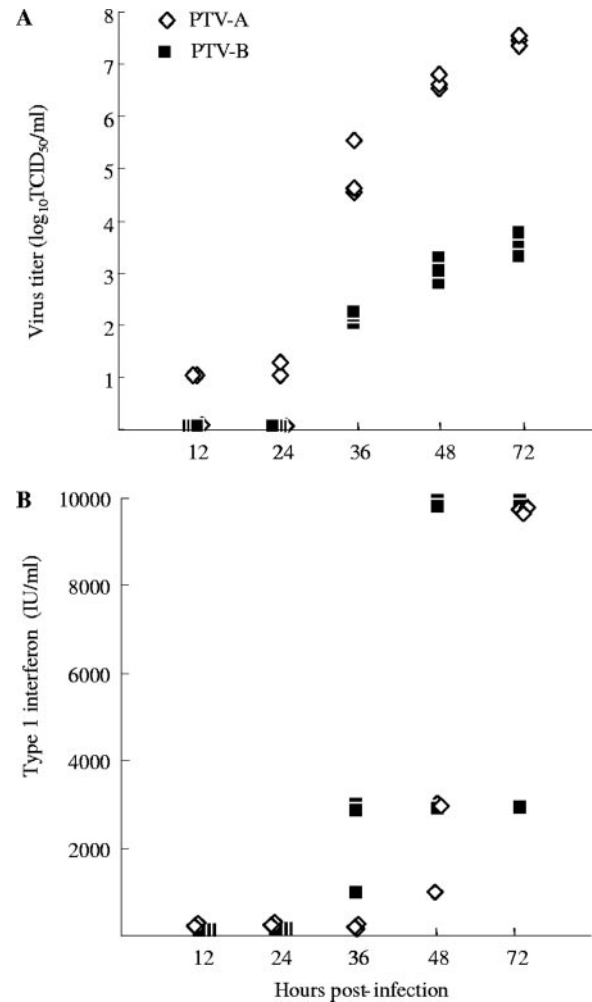
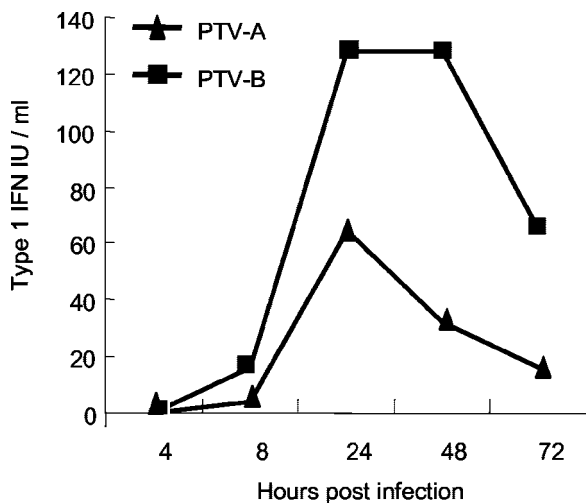


FIG. 4. Viremia and type I IFN induction in PTV-infected hamsters. Hamsters were infected with 4.7 log₁₀ PFU of PTV-A and PTV-B strains, three animals per time point were euthanized, and serum titers for virus and type I IFN were determined. (A) The PTV-A strain replicates to higher titers in infected animals than the PTV-B strain beginning 12 h p.i. and continues to exhibit superior growth, with final titers reaching 4 logs higher than PTV-B-infected animals (TCID₅₀). (B) Serum IFN is detectable at 36 h p.i. and is higher in more PTV-B-infected animals at 36 and 48 h p.i. than in PTV-A-infected animals.

PTV infection, we measured the concentration of IFN- α/β and virus in sera from PTV-infected hamsters (Fig. 4). Animals were infected intraperitoneally with 100 μ l of parental strains PTV-A and PTV-B (4.7 log₁₀ PFU). Three animals per time point were euthanized, and the titers of IFN α/β and virus in serum were determined as described. At all of the time points

genotype only at later time points. (B) If L and M are held constant at A/B/-, addition of the small RNA segment from either PTV strain has similar results to those shown in Fig. 3A. A/B/A exhibits comparable growth to that of the A/A/A genotype, and A/B/B growth resembles that of the B/B/B genotype, particularly at earlier time points. (C) Studies with the B/A/- background further demonstrate the in vitro growth advantage that the PTV-A S RNA segment confers.



CPE*

PTV-A	0	0	1	2	4
PTV-B	0	0	0	1	2

FIG. 5. Type I IFN induction in vitro by PTV strains. Primary HEFs were grown to confluence in T-25 flasks. Duplicate infections utilized an MOI of 1 of each PTV strain and Sendai as an induction control. Medium was sampled over time with replacement and treated for IFN titration as described. Titers of samples were determined for type I IFN by standard VSV plaque reduction assay on CHO cells and represented above as mean titers. *, CPE scores: 0, no cell death; 1, 25% cell death; 2, 50% cell death; 3, 75% cell death; 4, >90% cell death.

following infection, PTV-A-infected animals exhibited higher virus titers than PTV-B-infected animals (Fig. 4A). PTV-A was detected in serum as early as 12 h p.i., and virus titers reached 4.5 to 5.5 \log_{10} TCID₅₀/ml by 36 h p.i. In contrast, PTV-B virus replication was not detected until 36 h p.i. and was 2 logs lower than PTV-A titers at that time point. The PTV-B titers were approximately 3 to 4 logs lower than PTV-A strain at 48 and 72 h p.i. These data reflect the observed in vitro titers in HEFs (Fig. 3). After 72 h p.i., most hamsters infected with this dose of PTV-A strain have succumbed to infection.

Analysis of IFN- α/β levels in infected animals demonstrated a marked difference between PTV strains beginning at 36 h p.i. (Fig. 4B). Animals infected with the PTV-A strain had significantly reduced levels of IFN- α/β production at early time points compared with the PTV-B-infected animals. While IFN- α/β titers in both PTV-infected groups eventually reached similar levels at 72 h p.i., the late IFN levels in the PTV-A group can be attributed to the associated high levels of virus in organs (Fig. 4A). These data suggest that the PTV-A strain is more effective than the PTV-B strain in inhibiting the early induction of IFN- α/β response in vivo. This could allow the PTV-A strain to grow to higher titers in target organs, which could contribute to the high lethality of this strain.

The lethal PTV-A strain inhibits the induction of type I IFN in vitro. To assess the ability of the PTV-A strain to inhibit the induction of IFN- α/β in vitro, we examined whether the PTV-A and PTV-B strains exhibited a differential ability to induce IFN- α/β in primary HEFs. HEFs were infected with PTV-A and PTV-B virus at an MOI of 1. The culture supernatant was sampled at various times p.i., samples were acid-

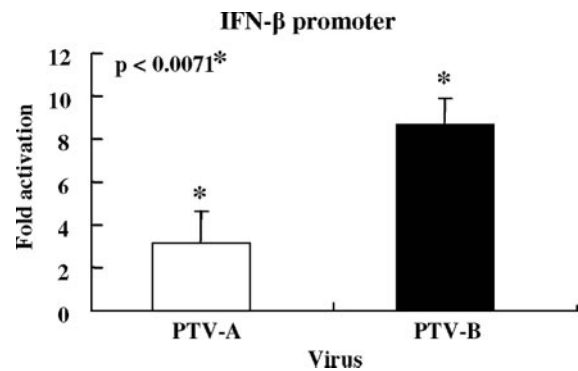


FIG. 6. Activation of the IFN- β promoter by PTV strains. 293 cells were transfected with reporter plasmids and infected 6 h posttransfection with an MOI of 3 of PTV strains (assays were performed in triplicate). Luciferase activity was measured from prepared lysates as described and normalized to β -Gal activity (expressed as relative [n-fold] induction). The PTV-B strain demonstrated a threefold-higher activation of the IFN- β promoter than the PTV-A strain. The difference in relative induction was statistically significant, as determined by Student's *t* test (*, $P < 0.0071$).

treated, and titers of IFN- α/β were determined by VSV plaque reduction assay on CHO cells (19). Beginning as early as 8 h p.i., the PTV-B strain induced measurable levels of type I IFN compared to the PTV-A strain (Fig. 5). PTV-B infection induced approximately two- to fourfold-higher levels of type I IFN than PTV-A infection at 24 and 48 h p.i., respectively. In addition, cells were observed for CPE during the course of the experiment, and PTV-A-infected cells showed more CPE and reached maximal CPE earlier than PTV-B-infected cells. The IFN- α/β titers in both PTV strain-infected cultures decreased by 72 h p.i., which could be attributed to the overall decrease in the number of viable cells in culture (CPE score = 4, which is >90% cell death).

To determine whether the PTV-A strain inhibits the transactivation of the IFN- β promoter, we examined the IFN- β promoter activity in PTV-infected cells using a luciferase reporter gene assay. The ability of the PTV-A and PTV-B strains to grow in 293 cells was confirmed previously by growth curve analysis (data not shown). Human 293 cells were transfected with the reporter plasmid, IFN- β -luc and subsequently infected with either PTV-B or PTV-A strain at an MOI of 3. The PTV-A stimulated the IFN- β promoter activity approximately threefold (luciferase activity normalized to β -Gal activity), whereas infection with the PTV-B strain resulted in ninefold stimulation (Fig. 6). Immunoprecipitation analysis using anti-PTV polyclonal antiserum showed that the level of expression of NSs and N proteins, encoded by the S segment, in PTV-infected 293 cells was similar for both PTV-A and PTV-B strains (data not shown). The difference in relative induction between the two PTV strains was found to be statistically significant ($P = 0.0071$). Collectively, these data indicated that the PTV-B strain is a better inducer of the IFN- β promoter than the PTV-A strain.

Next we examined whether the PTV NSs gene, encoded by the S segment, can inhibit stimulation of the IFN- β promoter in the absence of other viral proteins/factors. To test this possibility, we used a luciferase reporter assay to measure the ability of the expressed PTV NSs to inhibit the Sendai virus-

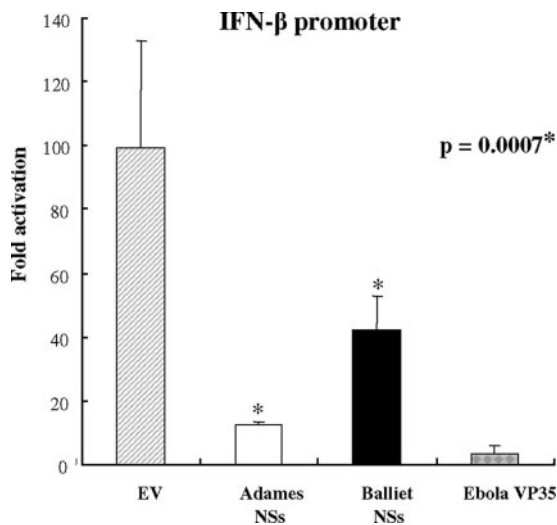


FIG. 7. Activation of the IFN- β promoter by PTV NSs. 293 cells were transfected with reporter and expression plasmids and infected 24 h posttransfection with 100 hemagglutinin units/ml of Sendai virus (assays were performed in triplicate). Cell lysates were prepared 18 h p.i., and luciferase activity was measured and normalized to β -Gal activity (expressed as relative [n -fold] induction). The PTV-A NSs demonstrated a threefold-greater inhibition of the IFN- β promoter activation than the PTV-B NSs. The difference in relative induction was statistically significant, as determined by Student's t test (*, $P = 0.0007$). EV, empty vector.

induced activation of the IFN- β promoter. The Ebola virus VP35 protein was used as a positive control (6). Sendai virus efficiently activated the IFN- β promoter in cells transfected with the negative control plasmid (Fig. 7, EV). As expected, the Ebola virus VP35 protein completely blocked the activation of the IFN- β promoter (Fig. 7). Expression of the PTV-A strain NSs significantly inhibited the activation of the IFN- β promoter, whereas PTV-B strain NSs showed a much weaker inhibition of the IFN- β promoter activation (Fig. 7). The PTV-A strain NSs inhibited IFN- β promoter activation approximately threefold more than the PTV-B strain NSs at high level of statistical significance ($P = 0.0007$). These results indicate that the PTV-A NSs protein encoded by the S genome segment is a type I IFN antagonist.

DISCUSSION

Recent outbreaks of *Phlebovirus*-induced disease around the world highlight the ability of viruses such as RVFV to invade previously naive regions where amplification hosts and vectors of transmission are becoming more abundant (11, 21, 26, 33, 40). There are currently no licensed human or veterinary vaccines or effective treatment measures for *Phlebovirus* disease. Effective animal systems to model and investigate mechanisms of human disease have been limited, with mice having recently been utilized to investigate *Phlebovirus* encephalitis, as seen in Toscana virus infections and the hemorrhagic fever manifestations of RVFV in mice and nonhuman primates (12, 24, 39).

Genetic reassortants have been utilized previously to investigate viral RNA segment-associated pathogenic factors in the *Bunyaviridae* family. Studies using reassortants produced between LaCrosse and snowshoe hare orthobunyaviruses impli-

cated the M RNA segment in encephalitis in mice (34). A study performed using reassortants generated between a RVFV deletion mutant (clone 13) and a wild-type virulent strain ZH548 to map genetic determinants for mouse virulence revealed that the S segment contained important elements for lethality (39). RVFV clone 13 has an in-frame deletion of approximately 70% of its NSs gene on the S RNA segment (25).

Previous studies of PTV-A infection of Syrian hamsters have shown rampant virus replication, with the liver as the major site of growth and also involvement of the duodenum and spleen (3). We confirmed these findings and also showed that the less pathogenic PTV-B had a similar pattern of growth but with less extensive tissue damage. The cause of death due to PTV infection is hemorrhagic shock from viral damage to the duodenal villi, and the shock probably contributes to the splenic damage and the centrolobular necrosis seen in some animals. The patterns of virus replication and the hepatic lesions resemble the pathogenesis of the *Phlebovirus* RVFV in experimental animals and in humans (4, 20, 24).

The PTV-A strain is also more virulent in the murine system than is the PTV-B strain, but the system must be carefully balanced with a selected age of the inbred mouse to demonstrate the difference (29). Interestingly, the mouse differences depend on age, and mice older than 5 weeks survive PTV-A strain infection. There are insufficient numbers of documented PTV-human infections to accurately understand the spectrum of illness elicited by each PTV strain.

Examination of several PTV strains suggests that the geographic origin of the isolate correlates with hamster pathogenicity (L. A. Perrone, unpublished observations). Viruses from the western part of Panama resemble PTV-B in their pathogenicity, and those from eastern Panama behave like PTV-A. This is independent of origin of the isolate (humans, sand flies, or sentinel animals) and of the passage history of the virus. Although the vertebrate amplifier in nature is unknown, we speculate that the difference in pathogenesis reflects different intraspecific or interspecific requirements for this host in the two geographic regions in which the contrasting phenotypes occur.

Utilizing reassortants generated between the lethal PTV-A strain (A/A/A genotype) (L/M/S RNA segment convention) and the nonlethal PTV-B strain (B/B/B genotype), we demonstrate that the S segment is a critical determinant of PTV virulence in hamsters, exemplified most prominently by the lethal phenotype of the B/B/A genotype and the nonlethal phenotype of the A/A/B genotype (Table 2). However, it was also found that the B/A/A and A/B/A genotypes exhibit a higher overall percentage of mortality in hamsters than the B/B/A genotype, suggesting a contribution of multiple RNA genome segments or their collective interaction to PTV pathogenesis. In other experiments performed by our group, we find that there is a preferential association during PTV replication and/or packaging in vitro between homologous M and S and between homologous L and S RNA segments (unpublished observations), which may explain why the B/B/A elicits a lower overall percent mortality in vivo than the other PTV genotypes containing the Adames S RNA segment. We hypothesize that whatever mechanism underlies the preferential association, it is operating doubly in this case and may put the B/B/A geno-

type at a slight disadvantage compared to the other lethal genotypes *in vivo*. Supporting this conjecture is the longer MTD observed in hamsters infected with the B/B/A genotype (5 to 7 days p.i.) than in the other lethal reassortant genotypes. It may not be coincidental that of all the reassortants with the PTV-A S RNA segment, B/B/A grew least well in HEF cells, and similarly, among the viruses bearing the PTV-B S RNA segment, A/A/B reached lower titers (Fig. 3). Importantly, no difference in tissue tropism was observed between any of the PTV genotypes, and the evidence indicates that lethality does not correlate with organ targeting.

The observed differences in the LD₅₀s between PTV-A and PTV-B strains, along with the observation that PTV-A titers rise rapidly within hours of infection (Fig. 4A), indicated that PTV-A strain might suppress the type I IFN response more efficiently than the PTV-B strain, resulting in an overwhelming infection and death in PTV-A-infected animals. Type I IFN (IFN- α/β) is an innate immune cytokine involved in viral clearance and paracrine cell signaling and is critical early during infection as an intercellular mediator to limit cell infection. Many viruses have evolved mechanisms to counteract the induction and/or action of IFN- α/β to propagate in the host and thrive in nature (15).

Among phleboviruses, the participation of IFN in pathogenesis was noted early in experimental studies of RVFV infections of mice (28); however, the first data implicating it in differences in pathogenesis came from studies of rat-pathogenic and non-rat-pathogenic virus strains. The strains capable of killing rats were much less sensitive to the antiviral effects of rat (but not human) IFN in cell culture (2). Studies of the IFN response and prophylaxis in rhesus monkeys are more directly relevant to pathogenesis of *Phlebovirus* infections (23). This model is the most realistic for human RVFV hemorrhagic fever, and prophylaxis with IFN- α was effective in suppressing disease and viremia. In untreated monkeys, there was a strong correlation between the timing (but not the magnitude) of the IFN response and the likelihood of disease or death; early responses were predictive of a mild clinical course and normal biochemical and clotting parameters.

We measured serum IFN- α/β levels *in vivo* following PTV challenge and found that the PTV-A strain fails to induce as robust an IFN- α/β response as the PTV-B strain, as demonstrated by IFN- α/β titers at critical early time points for hamster survival, specifically 36 and 48 h p.i. (Fig. 4B). While IFN- α/β titers in PTV-A and PTV-B infected animals eventually reach similar levels, we believe that the levels of circulating IFN in PTV-A-infected animals reflect their overwhelming viremia and presence of intracellular double-stranded RNA. *In vitro* experiments measuring IFN- α/β induction in cultured primary hamster embryo cells confirm our observations *in vivo* (Fig. 5). The serum IFN differences seen are important in two ways. First, IFN is detected earlier after inoculation of PTV-B into either cell cultures or surviving hamsters, which is a factor that was shown to be more important in the survival of RVFV-infected macaques than the actual titers elicited. In addition, in the case of PTV, the early IFN titers are higher for PTV-B than PTV-A. While both PTV strains and their reassortants were able to grow in IFN- α/β -competent (Fig. 3) as well as incompetent cells (Fig. 2), significant differences in growth over time are observed between genotypes in primary HEFs

(Fig. 3). It is clear that the presence of the PTV-A strain S RNA segment confers a growth advantage *in vitro* compared to those PTV reassortants containing the PTV-B S RNA segment.

Given the evidence that the PTV-A strain inhibits IFN- α/β production *in vivo* and *in vitro*, we determined the ability of the virus to suppress the transactivation of the IFN- β promoter using a reporter assay. The PTV-B strain stimulated the IFN- β promoter approximately threefold higher than the PTV-A strain (Fig. 6). Reporter assay experiments conducted using the lethal ZH548 and attenuated clone 13 strains of RVFV showed a fivefold difference between ZH548 and clone 13 in IFN- β promoter induction (7). It should be noted, however, that RVFV clone 13 is a virus obtained in the laboratory from a virulent RVFV strain and has a large (approximately 70%) in-frame deletion in the S RNA segment, resulting in a truncated NSs protein. The PTV-B strain is a naturally occurring isolate producing a full-length NSs protein. In the PTV S segment, there are no amino acid differences between the N proteins of PTV-A and PTV-B strains (GenBank accession no. DQ363406 and K02736 [16]). This implicated the NSs gene/protein in the observed differences between strains to elicit a type I IFN response and to stimulate the IFN- β promoter. To confirm this deduction, we performed IFN- β promoter-driven reporter assays and found that the PTV-A NSs gene/protein can independently inhibit the activation of the IFN- β promoter (Fig. 7). There are 13 amino acid differences between the PTV-A and PTV-B strains which would be ideal targets for site-directed mutagenesis and mapping of this protein's IFN-antagonistic ability. There is little amino acid sequence identity (27 common residues of an alignment of 250) between the RVFV and PTV NSs proteins, and it is currently unknown if the PTV NSs protein localizes to the nucleus (7, 35, 41).

Taken together, these results highlight the enhanced ability of the PTV-A strain to suppress the induction of type I IFN, allowing the virus to replicate more efficiently. These studies indicate that the PTV-A strain has a significant growth advantage over the PTV-B strain due to its ability to suppress the production of IFN- α/β via the action of the NSs protein early in infection, leading to uncontrolled viral replication in target tissues and, ultimately, host death. These results contribute significantly toward understanding of the mechanism of *Phlebovirus* pathogenesis in mammalian hosts.

ACKNOWLEDGMENTS

This work was sponsored in part by NIH contract grant NO1-AI-25489 (R.B. Tesh, principle investigator; C.J.P., coinvestigator). L.A.P. was supported by the McLaughlin Fund predoctoral fellowship in Infection and Immunity.

We thank Robert Tesh for the PTV Adames and Balliet strains and Juan Olano and Shu-Yuan Xiao for their assistance in histopathological examination of hamster tissues. We also thank Sam Baron and Joyce Poast for assistance in the development of a hamster species-specific IFN- α/β assay and James Grady, Shinji Makino, and Christopher Basler for their technical advice.

REFERENCES

- Ahmad, K. 2000. More deaths from Rift Valley fever in Saudi Arabia and Yemen. *Lancet* **356**:1422.
- Anderson, G. W. Jr., and C. J. Peters. 1988. Viral determinants of virulence for Rift Valley fever (RVF) in rats. *Microb. Pathog.* **5**:241-250.
- Anderson, G. W. Jr., M. V. Slayter, W. Hall, and C. J. Peters. 1990. Pathogenesis of a phleboviral infection (Punta Toro virus) in golden Syrian hamsters. *Arch. Virol.* **114**:203-212.

4. **Anderson, G. W. Jr., T. W. Slone, Jr., and C. J. Peters.** 1987. Pathogenesis of Rift Valley fever virus (RVFV) in inbred rats. *Microb. Pathog.* **2**:283–293.
5. **Bartelloni, P. J., and R. B. Tesh.** 1976. Clinical and serological responses of volunteers infected with phlebotomus fever virus (Sicilian type). *Am. J. Trop. Med. Hyg.* **25**:456–462.
6. **Basler, C. F., X. Wang, E. Muhlberger, V. Volchkov, J. Paragas, H. D. Klenk, A. Garcia-Sastre, and P. Palese.** 2000. The Ebola virus VP35 protein functions as a type I IFN antagonist. *Proc. Natl. Acad. Sci. USA* **97**:12289–12294.
7. **Billecocq, A., M. Spiegel, P. Vialat, A. Kohl, F. Weber, M. Bouloy, and O. Haller.** 2004. NSs protein of Rift Valley fever virus blocks interferon production by inhibiting host gene transcription. *J. Virol.* **78**:9798–9806.
8. **Bollin, E., Jr.** 1981. Production, partial purification, and characterization of Syrian hamster interferon. *Methods Enzymol.* **78**:178–181.
9. **Bouloy, M., C. Janzen, P. Vialat, H. Khun, J. Pavlovic, M. Huerre, and O. Haller.** 2001. Genetic evidence for an interferon-antagonistic function of Rift Valley fever virus nonstructural protein NSs. *J. Virol.* **75**:1371–1377.
10. **Braitto, A., M. G. Ciufolini, L. Pippi, R. Corbisiero, C. Fiorentini, A. Gistri, and L. Toscano.** 1998. Phlebotomus-transmitted Toscana virus infections of the central nervous system: a seven-year experience in Tuscany. *Scand. J. Infect. Dis.* **30**:505–508.
11. **Charrel, R. N., P. Gallian, J. M. Navarro-Mari, L. Nicoletti, A. Papa, M. P. Sanchez-Seco, A. Tenorio, and X. de Lamballerie.** 2005. Emergence of Toscana virus in Europe. *Emerg. Infect. Dis.* **11**:1657–1663.
12. **Cusi, M. G., S. G. Gori, C. Terrosi, G. G. Di, M. Valassina, M. Valentini, S. Bartolommei, and C. Miracco.** 2005. Development of a mouse model for the study of Toscana virus pathogenesis. *Virology* **333**:66–73.
13. **Fisher, A. F., R. B. Tesh, J. Tonry, H. Guzman, D. Liu, and S. Y. Xiao.** 2003. Induction of severe disease in hamsters by two sandfly fever group viruses, Punta toro and Gabek Forest (Phlebovirus, Bunyaviridae), similar to that caused by Rift Valley fever virus. *Am. J. Trop. Med. Hyg.* **69**:269–276.
14. **Griot, C., A. Pekosz, D. Lukac, S. S. Scherer, K. Stillmock, D. Schmeidler, M. J. Endres, F. Gonzalez-Scarano, and N. Nathanson.** 1993. Polygenic control of neuroinvasiveness in California serogroup bunyaviruses. *J. Virol.* **67**:3861–3867.
15. **Haller, O., G. Kochs, and F. Weber.** 2006. The interferon response circuit: induction and suppression by pathogenic viruses. *Virology* **344**:119–130.
16. **Ihara, T., H. Akashi, and D. H. Bishop.** 1984. Novel coding strategy (ambisense genomic RNA) revealed by sequence analyses of Punta Toro *Phlebovirus* S RNA. *Virology* **136**:293–306.
17. **Ihara, T., J. Smith, J. M. Dalrymple, and D. H. Bishop.** 1985. Complete sequences of the glycoproteins and M RNA of Punta Toro *Phlebovirus* compared to those of Rift Valley fever virus. *Virology* **144**:246–259.
18. **Janssen, R. S., N. Nathanson, M. J. Endres, and F. Gonzalez-Scarano.** 1986. Virulence of La Crosse virus is under polygenic control. *J. Virol.* **59**:1–7.
19. **Langford, M. P., D. A. Weigent, G. J. Stanton, and S. Baron.** 1981. Virus plaque reduction assay for interferon: microplaque reduction assays, p. 330–346. *In* S. Petska (ed.), *Methods in enzymology*. Academic Press, New York, NY.
20. **Laughlin, L. W., J. M. Meegan, L. J. Strausbaugh, D. M. Morens, and R. H. Watten.** 1979. Epidemic Rift Valley fever in Egypt: observations of the spectrum of human illness. *Trans. R. Soc. Trop. Med. Hyg.* **73**:630–633.
21. **Linthicum, K. J., A. Anyamba, C. J. Tucker, P. W. Kelley, M. F. Myers, and C. J. Peters.** 1999. Climate and satellite indicators to forecast Rift Valley fever epidemics in Kenya. *Science* **285**:397–400.
22. **Meegan, J. M., R. J. Yedloutschnig, B. A. Peleg, J. Shy, C. J. Peters, J. S. Walker, and R. E. Shope.** 1987. Enzyme-linked immunosorbent assay for detection of antibodies to Rift Valley fever virus in ovine and bovine sera. *Am. J. Vet. Res.* **48**:1138–1141.
23. **Morrill, J. C., G. B. Jennings, T. M. Cosgriff, P. H. Gibbs, and C. J. Peters.** 1989. Prevention of Rift Valley fever in rhesus monkeys with interferon-alpha. *Rev. Infect. Dis.* **11**(Suppl. 4):S815–S825.
24. **Morrill, J. C., G. B. Jennings, A. J. Johnson, T. M. Cosgriff, P. H. Gibbs, and C. J. Peters.** 1990. Pathogenesis of Rift Valley fever in rhesus monkeys: role of interferon response. *Arch. Virol.* **110**:195–212.
25. **Muller, R., J. F. Saluzzo, N. Lopez, T. Dreier, M. Turell, J. Smith, and M. Bouloy.** 1995. Characterization of clone 13, a naturally attenuated avirulent isolate of Rift Valley fever virus, which is altered in the small segment. *Am. J. Trop. Med. Hyg.* **53**:405–411.
26. **Peters, C. J.** 1997. Emergence of Rift Valley fever, p. 253–264. *In* J. F. Saluzzo and B. Dodet (ed.), *Factors in the emergence of arbovirus diseases*. Elsevier, Paris, France.
27. **Peters, C. J., and J. M. Meegan.** 1981. Rift Valley fever, p. 403–419. *In* G. Beran (ed.), *CRC handbook series in zoonoses*. CRC Press, Inc., Boca Raton, FL.
28. **Peters, C. J., and T. W. Slone.** 1982. Inbred rat strains mimic the disparate human response to Rift Valley fever virus infection. *J. Med. Virol.* **10**:45–54.
29. **Pifat, D. Y., and J. F. Smith.** 1987. Punta Toro virus infection of C57BL/6J mice: a model for phlebovirus-induced disease. *Microb. Pathog.* **3**:409–422.
30. **Sabin, A. B., C. B. Philip, and J. R. Paul.** 1944. Phlebotomus (papatasi or sandfly) fever. A disease of military importance: summary of existing knowledge and report of original investigations. *JAMA.* **125**:603–606, 697–699.
31. **Sabin, A. B.** 1951. Experimental studies on phlebotomus (pappataci, sandfly) fever during World War II. *Arch. Gesamte Virusforsch.* **4**:367–410.
32. **Seth, R. B., L. Sun, C. K. Ea, and Z. J. Chen.** 2005. Identification and characterization of MAVS, a mitochondrial antiviral signaling protein that activates NF-kappaB and IRF 3. *Cell* **122**:669–682.
33. **Shope, R. E., C. J. Peters, and F. G. Davies.** 1982. The spread of Rift Valley fever and approaches to its control. *Bull. W. H. O.* **60**:299–304.
34. **Shope, R. E., E. J. Rozhon, and D. H. Bishop.** 1981. Role of the middle-sized bunyavirus RNA segment in mouse virulence. *Virology* **114**:273–276.
35. **Struthers, J. K., and R. Swanepoel.** 1982. Identification of a major non-structural protein in the nuclei of Rift Valley fever virus-infected cells. *J. Gen. Virol.* **60**:381–384.
36. **Tesh, R. B.** 1988. The genus *Phlebovirus* and its vectors. *Annu. Rev. Entomol.* **33**:169–181.
37. **Tesh, R. B., C. J. Peters, and J. M. Meegan.** 1982. Studies on the antigenic relationship among phleboviruses. *Am. J. Trop. Med. Hyg.* **31**:149–155.
38. **Tesh, R. B., S. Saidi, S. J. Gajdamovic, F. Rodhain, and J. Vesenjak-Hirjan.** 1976. Serological studies on the epidemiology of sandfly fever in the Old World. *Bull. W. H. O.* **54**:663–674.
39. **Vialat, P., A. Billecocq, A. Kohl, and M. Bouloy.** 2000. The S segment of Rift Valley fever *Phlebovirus* (*Bunyaviridae*) carries determinants for attenuation and virulence in mice. *J. Virol.* **74**:1538–1543.
40. **World Health Organization.** 2000. Rift Valley fever, Saudi Arabia, August–October 2000. *Wkly. Epidemiol. Rec.* **75**:370–371.
41. **Yadani, F. Z., A. Kohl, C. Prehaud, A. Billecocq, and M. Bouloy.** 1999. The carboxy-terminal acidic domain of Rift Valley Fever virus NSs protein is essential for the formation of filamentous structures but not for the nuclear localization of the protein. *J. Virol.* **73**:5018–5025.